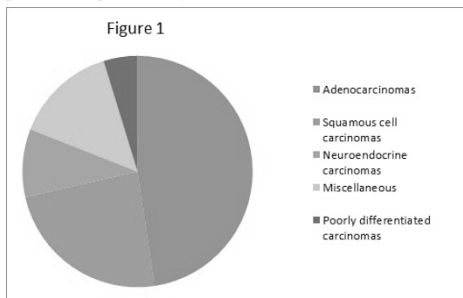using a 10x objective. IHC is highly sensitive for NTM but has a lower sensitivity for *MTB*, suggesting that cases with a high clinical suspicion for *MTB* should be sent for PCR even when AFB and IHC are negative.

1578 Morphologic Characterization of Incidentally Discovered Granulomas in Lung Neoplasms
Neelima Valluru, Swati Mehrotra, Stefan Pambuccian, Vijayalakshmi Ananthanarayanan. Loyola University Medical Center, Maywood, IL.
Background: Granulomatous reaction to tumor is an unusual phenomenon and has been described within main tumor or in the draining lymph nodes. Lung is commonly involved by granulomatous lesions of various infectious and non-infectious etiologies. Co-existence of granulomatous inflammation in lung tumors may pose diagnostic difficulties and may influence therapeutic decisions. The aim of the study is to identify and describe the morphological patterns of granulomatous inflammation seen in association with lung neoplasms
Design: This single institutional retrospective study from 2001 to 2015 identified 42 lung resection specimens of lung cancers with coexisting granulomatous inflammation.
Results: The median age of the patients was 58 years of whom 65.2% were males. Majority of the cases were lobectomies (n=40); followed by pneumonectomies (n=2). All 42 cases had granulomas within the adjacent lung parenchyma. None of the cases elicited a granulomatous response within tumor stroma. Of these, 5 cases also had granulomatous involvement of the draining lymph nodes without evidence of metastasis. Several morphologic types of granulomas were encountered: Hyalinized (45.2%), calcified (23.8%) and necrotizing (31%). GMS stain identified Aspergillus and Histoplasma as the infectious cause of necrotizing granulomas in 2 of the cases. AFB stain was negative in all the cases. The distribution of the granulomas across subtypes of lung neoplasms is depicted in figure 1.

Figure 1

- Adenocarcinomas
- Squamous cell carcinomas
- Neuroendocrine carcinomas
- Miscellaneous
- Poorly differentiated carcinomas

Tumors metastatic to the lung were included under miscellaneous.
Conclusions: In our study set across 15 years, we found that most of the granulomas associated with lung neoplasms are noted to be of non-infectious etiology. It is not clear whether granulomas in association with lung neoplasms and draining lymph nodes, are of any prognostic significance; It is likely that these may represent an aberrant immunological response to tumor related antigens. Being in a histoplasma endemic region, the infectious etiology in necrotizing granulomas still has to be ruled out by PCR testing.

1579 Primary Syphilis in the Tonsil: Challenges in Histopathological Diagnosis
Cheng-Han Yang, Ting-Yi Su, Kai-Ping Chang, Li-yu Lee. Linkou Chang Gung Memorial Hospital, Taoyuan, Taiwan.
Background: Primary syphilis usually appears on the genitalia, but may present on other sites such as anus or oral cavity. There have been 12 cases of tonsillar primary syphilis published in English literature. Most of them had sufficient clinical information prior to the diagnostic tests, and detailed pathological information was not provided. We describe an additional case with challenging pathological diagnosis due to lack of clinical information.
Design: We report a 30-year-old man with the chief complaint of sore throat for one week. His right tonsil showed grade IV swelling with an ulcerative surface. A biopsy was performed. The tissue was formalin-fixed and paraffin embedded. Hematoxylin and eosin stained slides were reviewed and further immunohistochemical studies were performed.
Results: Microscopically, the tonsillar tissue showed ulcerated squamous epithelium with fibrinopurulent exudates and reactive keratinocytic atypia. The underlying connective tissue and lymphoid nodules showed heavy infiltrations of plasma cells, lymphocytes and histiocytes. Perivascular plasmalymphocytic infiltrations and endarteritis are seen. Immunohistochemically, there was no light chain restriction by kappa and lambda immunostains. The plasma cells are diffusely positive for IgG, but only focally positive for IgG4. Periodic acid-Schiff stain and acid-fast stains showed no fungal or mycobacterial infection. Finally, numerous *Treponema pallidum* were detected by anti-*T. pallidum* antibody in the squamous epithelium, submucosa, and vessel walls. After pathologically diagnosis of a primary syphilis, serologic tests were performed. The Rapid Plasma Reagin test was reactive at 1:128, and the *Treponema Pallidum* Particle Agglutination test showed reactive at > 1:1280. As a result, the diagnosis of primary syphilis was confirmed.
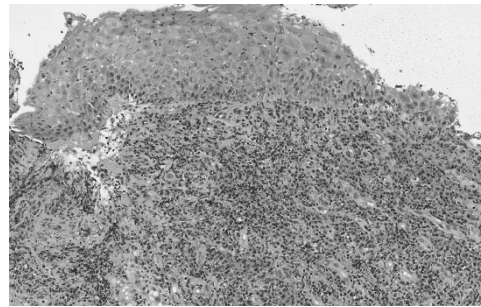
Conclusions: Pathological diagnosis of primary syphilis may be challenging without sufficient clinical information, because the microscopic features are not specific. A tentative diagnosis can be made by combination of clinical information and microscopic findings, and serologic tests are needed for confirmation.

Informatics

1580 The Automatic Extraction and Categorization of 11,347 Large Bowel Polyps from 54,631 Free Text Surgical Pathology Reports
Michael Bonert, Jennifer M Dmetrichuk, Asghar Naqvi. McMaster University/St. Joseph's Healthcare Hamilton, Hamilton, ON, Canada.
Background: Observational data is commonly used in process management in clinical pathology and manufacturing; however, anatomic pathology data related to pre-cancerous conditions is not routinely assessed to extract trends and gauge the variation due to health care providers.
Design: All surgical pathology reports (54,631) for a 3 year period, in a large academic center, were data-mined using a custom computer program to extract all large bowel polyp specimens. Diagnostic information including the anatomic location was categorized using keyword searches, an approximate string matching library (google-diff-match-patch), and hierarchical pruning. The categorizations by the computer were compared to pathologist reads for a random subset of reports to assess accuracy.
Results: 53,967 (98.8%) of the complete reports were successfully parsed into individual specimen parts, and 11,457 large bowel polyp specimens were extracted. 68 cases with large bowel polyps could not be parsed, due to unusual report formatting (37), mislabelled parts (24), and missing specimens parts (7). 11,347 (99%) of large bowel polyps were diagnostically classified, and human reads of a randomly selected subset of 200 specimens demonstrated that the computer's diagnostic categorization was correct >98% of the time. Using the parsed output, the tissue acquired and diagnostic interpretation were stratified by the submitting endoscopist and the signing pathologist using a spreadsheet (Microsoft Excel). Completeness of the clinical history could be stratified by submitting endoscopist. The program could successfully parse and extract a large number of reporting styles; however, it failed more frequently when parts were lumped or when the reporting style significantly deviated from Association of Directors of Anatomic and Surgical Pathology recommendations.
Conclusions: The automatic extraction and categorization of diagnostic information in free text pathology reports is feasible and yields a large quantity of information that can be easily analysed. Pathologist reporting style may be a modifiable factor that could further improve analyses of this type. Routine analyses of observational data for pre-cancerous conditions may facilitate (1) a greater understanding of the pathobiology in the served population, (2) factors important for optimization of care, and (3) improved cancer prevention and early cancer detection.

1581 A Synoptic Electronic Order Set for Placental Pathology: A Framework Extensible to Non-Neoplastic Pathology
Adela Cimic, S Joseph Sirintrapun. Maimonides Medical Center, Brooklyn, NY; Memorial Sloan Kettering Cancer Center, New York, NY.
Background: Synoptic reporting templates in neoplastic specimens are deemed crucial for quality patient care through comprehensive pathology reporting.Overlooked however is how pathology reporting suffers when there is omission of important clinical information prior to the pathologic evaluation.Particularly with non-neoplastic specimens like placental, renal, and liver;availability of certain curated clinical data elements are critical to obtaining the most accurate diagnosis.For instance historically paper requisitions in placental pathology allow for omission of clinical data or vague over-generalized histories such as "intrauterine pregnancy",which add nothing to help the pathologic assessment.
Design: With widespread adoption of electronic medical records,opportunities arise for electronic order sets (EOS) that ensure capture and availability of discrete clinical data.Currently however,no frameworks for EOS exist in anatomic pathology.Thus through clinical and pathologic curation via collaboration between the clinical teams and pathology,we have constructed an EOS for placental specimens.Many data elements are optional but included in our EOS are mandatory and critical data elements.

Results:

```
Page 1
MATERNAL INFORMATION
_____Gravida                              <optional>
_____Parity                               <optional>
Gestational age: _____    wks            <Mandatory><Numeric>
_____CHTN                                 <optional>
_____Preeclampsia                         <Critical>
_____Diabetes                             <optional>
_____GDM                                  <optional>

ANTEPARTUM:                                <optional>
_____IUGR                                 <Critical>
_____Polyhydramnios
_____Oligohydramnios
_____Infection crucial
_____In utero therapy
_____Stillbirth crucial
_____Fetal Hydrops
_____Multiple gestations
_____Single umbilical artery
_____Placenta previa
_____Congenital abnormalities
_____Poor obstetric history

INTRAPARTUM                                <optional>
_____Chorioamnionitis
_____NRFHT
_____Placental abruption                  <Critical>
_____Thick meconium|
_____FTP
_____Malpresentation

Page 2

DELIVERY:                                  <Mandatory>
_____Vaginal
_____Forceps/vacuum
_____Cesarean

NEONATE:
Baby A
Apgars :  ____1 minute  _____5 minutes     <Mandatory><Numeric>
_____Grossly normal                       <optional>
Malformations:_____  <---------------------> <optional><Free Text>

If twins or more  <--------------------->  <Expanding/collapsing menu>
Baby B
Apgars :  ____1 minute  _____5 minutes     <Mandatory><Numeric>

if twins please add Baby B
_____Grossly normal                       <optional>
Malformations:_____  <---------------------> <optional><Free Text>

INDICATIONS FOR PATHOLOGY REVIEW; SUMMARY:  <optional>
_____Chorioamnionitis
_____Hypertension
_____Diabetes
_____Abruption
_____IUGR
_____Oligohydramnios crucial to know
_____Polyhydramnios
_____Thick Meconium
_____Poor history
_____In utero therapy
_____Stillbirth
_____Pre-term
_____Post-term
_____<5 apgar at 1 min or pH7.2
_____Fetal Hydrops
_____Congenital anomalies
_____Multiple gestations
_____Single umbilical artery
_____Artery placental abnormality (velamentous cord inserion, vasa previa)
```

Figure 1 illustrates our EOS which captures mandatory necessary elements(red) such as gestational age for reporting.Critical elements(yellow)such as IUGR serve as decision support,to remind the importance of knowing that particular element for increased accuracy of reporting.The EOS accommodates workflow and enables for future data searches of clinical information.It provides a hierarchical framework amenable for translation to XML for data interoperability.This most useful advantage serves as a powerful research tool for residents, fellows, and motivated pathologists for future projects.

Conclusions: Our EOS by including mandatory,critical,and optional data elements;optimizes pathologic assessment and potentially averts catastrophic errors in placental pathology assessment.We intend for future rollouts of analogous EOS for renal and liver pathology.We propose that such EOS frameworks are necessary adoptions to enable quality pathologic reporting,particularly for non-neoplastic pathologic assessment.

1582   Design and Development of a 3D-Printed Apparatus to Hold a Smartphone for Histologic Examination and Associated Applications
Jesse Cox, Nicholas Lintel, Alexander L Braun, Audrey J Lazenby, Benjamin J Swanson. University of Nebraska Medical Center, Omaha, NE.
Background: Digital imaging and video capture are poised to revolutionize the practice of pathology and education. However, high capital costs for slide scanners and remote access devices have limited the widespread deployment within many pathology groups. Further, these high costs delay the upgrade cycle, often resulting in the use of inferior hardware and out-of-date software. In contrast, modern smartphones feature sophisticated cameras and integrated communication software, which are updated regularly. Moreover, these technologies are inexpensive and widely distributed. Thus, the use of a smartphone in lieu of more expensive remote scanning technology may open opportunities for smaller pathology practices to adopt imaging hardware and software for little cost. While devices currently exist to mount a smartphone to a microscope eyepiece, these devices have a steep learning curve, requiring adjustment in 6-axes (X, Y, Z, yaw, pitch, roll) to properly align the both the device and smartphone to the eyepiece. Thus, device setup can take a significant amount of time.
Design: To address these shortcomings, we designed and developed a 3D-printed mount using computer assisted drafting software, to quickly mount an iPhone to a microscope with only one axis of adjustment needed to properly orient the iPhone to capture images. As shown in the figure below, the mount slips around the outside of the left eyepiece snugly and has a shelf to hold the iPhone in position. A ledge cantilevers the device against the adjacent eyepiece to hold the mount level. This mount may also be adapted to fit a variety of microscopes and smartphones.

Results: We developed an apparatus that can be manufactured inexpensively (<$20), tailored specifically for an iPhone 6S+ and Olympus WHN10X/22 eyepiece. We highlight scenarios and provide evidence of the effectiveness of the iPhone mount/iPhone for remote cytology adequacy assessment, remote frozen section consultation, and slide scanning using built in software tools in iOS and popular image editing software.
Conclusions: We demonstrate a low-cost method for the wide deployment of digital microscopy that may have widespread application in the clinic, the laboratory and in the classroom.

1583   A Large Multicenter, Retrospective Non-Inferiority Study to Evaluate Diagnostic Concordance Between Optical vs Digital Microscopic Diagnoses in 2000 Surgical Pathology Cases
Michael Feldman, Brian P Rubin, Christopher A Moskaluk, Nicolas Cacciabeve, Guy Lindberg, Mischa Nelis, Clive R Taylor. Univ. Pennsylvania, Philadelphia, PA; Cleveland Clinic, Cleveland, OH; Univ. Virginia, Charlottesville, VA; Advanced Pathology Assoc, Rockville, MD; Miraca Life Science, Irving, TX; Philips Digital Pathology Solutions, Best, Netherlands; Univ. Southern California, Los Angeles, CA.
Background: Prior studies comparing diagnoses using digital vs optical microscopy have been small studies, sampling a single organ or lacking central adjudication. The objective of this study was to demonstrate that diagnosing surgical pathology slides with Philips Intellisite Digital Pathology Solution (PIPS) was non-inferior to using an optical microscope. Secondary objectives included comparison of manual digital (MD) and manual optical (MO) discordance rates for organs, subtypes and pathologists.
Design: A non-inferiority study design was used to compare MO vs MD reads of 2000 surgical pathology cases from 20 different organ systems (54 subtypes) with 16 reading pathologists from 4 institutions. A central adjudication charter was used by three independent pathologists to evaluate the MD and MO reads against the original main sign out diagnosis with scoring of no discordance, minor discordance or major discordance. The MD method will be declared non-inferior to the MO method if the upper bound of the 95% two-sided confidence interval for the MD – MO difference in error rate was less than 4%.
Results: A total of 1992 cases were included in the Full Analyses Set with 15,925 readings. The study determined an MD major discordance rate of 4.7%, an MO major discordance rate of 4.4%, and an MD-MO rate difference of 0.4% with a 95% confidence interval of (-0.30%; 1.01%) indicating non-inferiority for digital vs optical reads. Analysis by pathologist showed that for 14 out of 16 individual readers the difference between MD and MO was also below the pre-specified non-inferiority margin of 4%. By organs, the differences in major discordance rate between MD and MO were <2% in absolute value overall for all organs with prostate showing the highest major discordance rates of 12% MD and 11.3% MO. From the 54 subtypes, 20 sub-types demonstrated 0% difference between MD & MO while 31 subtypes had a difference between – 4% and +4%.
Conclusions: This study demonstrates that viewing and diagnosing surgical pathology tissue slides by using the Philips Digital Pathology System was non-inferior compared to optical microscopy.

1584   Area of Interest Analysis of Eye Gaze on Digital Pathology Media
Sharon Fox, Beverly E Faulkner-Jones. Beth Israel Deaconess Medical Center, Boston, MA.
Background: Digital pathology allows for the diagnosis of slide-based specimens in an electronic format. Prior work has utilized eye-tracking technology to study different forms of diagnostic visual processing. Eye-tracking enables the visualization of the gaze of the viewer, and analysis of this data is then performed on selected areas of interest (AOIs) within the digital image. To date, many different approaches to AOI selection have been employed for eye-tracking analysis. The methods of selecting AOIs in each diagnostic scenario are critical to interpretation of study results, and the accurate modeling of image data for computer-assisted diagnosis. We therefore compared several methods of area of interest selection as applied to the use of digital pathology.
Design: Pathologists were recruited to view a variety of digital pathology media, including static images and whole slide images (WSIs), with specimens presented in an image diagnosis task. WSIs were digitized on a Philips UFS scanner then viewed on SlideAtlas (https://slide-atlas.org), a high-performance web-based digital pathology system. Participants were instructed to explore the images in each format and render a diagnosis. A Tobii X2-60 eyetracker was used to collect gaze pattern data throughout the course of the experiment. In addition, participants and expert pathologists were asked to manually define areas of diagnostic interest (AOIs) within the images. These areas were defined on both the images in static form, as well as in dynamic form across the time of exploration of WSIs. The eye-tracking data acquired and analyzed included fixation count and duration. Analyses utilized participant-defined static AOIs, dynamic AOIs, and clustering of fixations.

Results: A comparison of manual AOI selection to clustering of fixations revealed significant differences between participants, with a high level of variability, and a positive correlation of manual selection and fixation clusters within individual participant data. In addition, results derived from analyses across dynamic AOIs were significantly different from those derived from defined static AOIs – even when using the same participant data.

Conclusions: The information gained through eye-tracking data can allow us to improve digital pathology media, as well as our understanding of image features relevant to diagnosis. Here we examine the effect of AOI selection methods on the results of eye-tracking data interpretation. The results of these studies may be useful in the computer selection and analysis of diagnostically relevant areas of interest on digital pathology images.

1585 Apply a Confocal WSI Scanner for FISH Slides Imaging, 3D Reconstruction, and Semi-Automated Diagnosis

Xiujun Fu, Pinky Bautista, Jochen K Lennerz, Maristela Onozato, Anthony Iafrate, Yukako Yagi. Massachusetts General Hospital, Boston, MA; Harvard Medical School, Boston, MA.

Background: Technological advances contribute to a maturation of digital pathology in clinical applications. However, there are few reports on confocal fluorescence imaging technology for whole-slide imaging (WSI). Here, we explored benchmark features of a confocal scanner for application in typical research and diagnostic imaging applications of fluorescence in situ hybridization (FISH) testing.

Design: Multi-layer (both Z-stack and extended focus) and single-layer modes were used with the Pannoramic Confocal scanner (3DHISTECH, Hungary) to digitize 20 FISH slides (EGFR-MET, HER2, and ALK). The objective used was 40× water immersion with a resolution of 0.1625 μm/pixel. Multiple layers scannings were setup with 6, 13, and 26 layers with 1, 0.4, and 0.2 μm interval respectively. Scanning time and file size were recorded. The 3D reconstruction, quantification of dots, and co-localization analysis were made with Imaris (Bitplane, Switzerland).

Results: Z-stack scanning increased the detection of intra-nuclear dots with the inclining of total number of scanned layers (no significant difference between 13- and 26-layer), although it increased scanning time and image file size (Fig 1A). Compared to Z-stack, the quantification analysis of dots showed extended focus decreased the number of dots, and the co-localization analysis of dots in different channels indicated extended focus increased the number of co-localized dots (Fig 1B-F).

A	1-layer	6-layer	13-layer	26-layer
FITC	132.6±29.3	158.1±26.9	173.8±41.9	170.4±43.2
TRITC	127.0±21.8	154.1±19.3	163.4±21.0	162.9±23.2
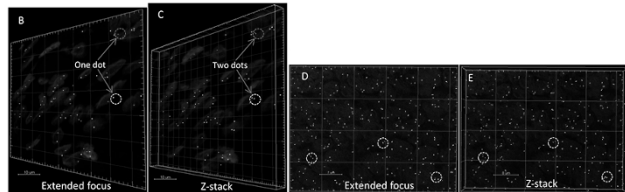
F	Z-stack			Extended focus		
	Co-localized	Total	Ratio(%)	Co-localized	Total	Ratio(%)
FITC	240.5±28.9	322.6±32.9	74.48±3.77	233.9±29.3	306.9±33.0	76.11±2.93
TRITC	241.3±29.0	370.9±32.6	64.97±4.31	238.4±31.2	357.1±30.9	66.58±4.46

Multiple channels allow to image various fluorophores simultaneously, and the numbers of dots and co-localized dots were analyzed automatically to support diagnosis of gene amplification, deletion, and fusion (Fig 2).
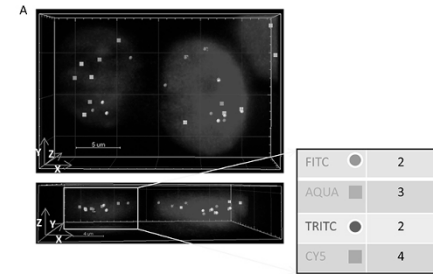
	FITC			TRITC			
Nuclei	Co-localized	Non-co-localized	Total	Co-localized	Non-co-localized	Total	Impression
1	1	3	4	1	2	3	+
2	1	2	3	2	1	3	+
3	1	2	3	1	0	1	-
4	0	2	2	0	1	1	+
5	0	3	3	0	1	1	+
...							

Conclusions: Multi-layer Z-stack scanning improves detection of intra-nuclear dots, although increases scanning time and storage. We foresee confocal Z-stack scanning as a tool for FISH imaging, and diagnosis supporting with automated analysis.


1586 Redefining the High Power Field When Counting Mitoses Using Digital Pathology

Matthew G Hanna, Liron Pantanowitz. UPMC, Pittsburgh, PA.

Background: Grading various neoplasms such as breast carcinoma, neuroendocrine tumors, and sarcomas includes an evaluation of mitotic count. Using glass slides, mitotic count is typically determined using 10 high power fields (HPF) at 40x magnification. In the era of digital pathology, several factors (e.g. image viewer, display) may affect mitotic scores. The aim of this study was to determine which hardware and software parameters may influence mitotic counts when reviewing whole slide images (WSI).

Design: A WSI calibration slide with 0.005 and 0.01mm markers was scanned at 20x (0.5 microns/pixel) and 40x (0.25 microns/pixel) on an Aperio ScanScopeXT and Hamamatsu Nanozoomer. Both scanners use an Olympus UPlanSAPO 20x/0.75 microscope objective. Digital slides were viewed (ImageScope and NDP viewer) with 5 screen resolutions: 1680x1050 (8:5), 1920x1080 (16:9), 1920x1200 (8:5), 2560x1440 (16:9), and 3840x2160 (16:9). Measurements were compared to a glass slide microscopic HPF area (0.196mm^2) at 40x magnification.

Results: No differences in field area were identified when scanning at 20x or 40x. Glass slide HPF at 40x magnification was not equal to 40x digital field areas.
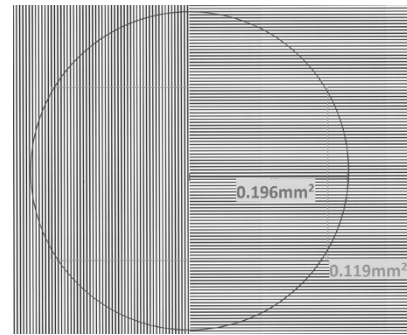
Comparison of microscope HPF (circle) to digital HPF (rectangle)

A 40x field of view with ImageScope, 0.136 mm^2 area, was equivalent to 69% microscope HPF. The NDP viewer, 0.119 mm^2 area, equaled 61% microscope HPF. Different screen resolutions produced different field areas (range 53-266%) relative to the glass slide HPF.

Screen resolution effect on HPF area at 40x digital magnification

Screen Resolution	Digital HPF Area (mm2)	WSI:Glass slide HPF
1680x1050	0.104	53%
1920x1080	0.123	63%
1920x1200	0.136	69%
2560x1440	0.220	112%
3840x2160	0.521	266%

There was a 9% field area difference using the same viewer to display different WSI file types of the same image.

Conclusions: Mitotic counting in digital pathology differs from that performed with glass slides. These data show that mitotic counts can vary with WSI due to differences in digital area displayed by image viewers, screen resolutions, and WSI file formats. To address these differences, mitotic scores for tumors attained on WSI may need to be standardized by predefined field areas that are equivalent to glass slide HPF measurements.


1587 Multiple Use Cases for Microsoft HoloLens in Pathology

Matthew G Hanna, Ishtiaque Ahmed, Shyam Prajapati, Jeffrey S Nine, Clayton Wiley, Liron Pantanowitz. UPMC, Pittsburgh, PA; Mount Sinai Hospital, New York, NY.

Background: Augmented Reality (AR) devices such as the Microsoft HoloLens have not been well utilized in the medical field. The HoloLens is a wearable, head-mounted computer that projects an interactive holographic image into the user's point-of-view. These holograms can be controlled by gaze, hand gesture and voice commands. Our aim was to test the HoloLens for educational and clinical applications in pathology.

Design: A Microsoft HoloLens (Developer Edition) was connected to the Internet via our institution's secure wireless network. Skype Beta for HoloLens was used for live streaming and bidirectional virutal annotation. Microsoft Edge web browser with various image viewers was employed for remote navigation of digital slides. Use cases included virtual annotation during autopsy, viewing 3D gross pathology specimens captured with a Shining3D Einscan-S 3D scanner, telepathology during frozen sections and from the gross work station, and whole slide image (WSI) viewing. AR sessions were captured using a Microsoft Surface Pro 3 tablet.

Results: Trainees performing an autopsy with the HoloLens were remotely instructed using real-time diagrams, annotations and voice instructions. Gestures and voice commands allowed organ weights, notes, and photographs to be recorded. 3D scanned gross pathology specimens could be viewed as holograms and easily manipulated (Figure 1a). During gross exam or intraoperative consultation, users could remotely access a pathologist for guidance, be provided ancillary material (i.e. radiology images), and annotate areas of interest on specimens in real-time. WSI were easy to remotely view and navigate using an AR workstation (Figure 1b).
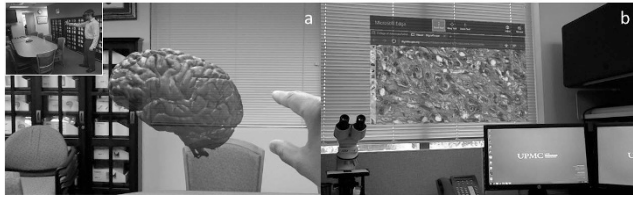
Augmented reality uses of the Microsoft HoloLens. (A) Holographic 3D scanned human brain interaction. (B) Remote viewing of WSI for telepathology.

Conclusions: The HoloLens is a novel tool that has multiple applications for pathology practice and education. The device was comfortable to wear, easy to use, and supported high resolution imaging. We were able to demonstrate that the HoloLens has multiple uses during autopsy, gross pathology and microscopic examination. Specific applications include remote supervision, annotation, recording, 3D and WSI viewing, and telepathology in a mixed-reality environment.

1588 Improving Workflow Efficiency for Special Stains in a Digital Pathology Laboratory
*Matthew G Hanna, Liron Pantanowitz, Megan Morrell, Katie Beseler, Jessica Stinner, Jon Duboy, Matthew O'Leary, Michael A Nalesnik, Douglas Hartman.* UPMC, Pittsburgh, PA.
Background: Digital pathology has tremendous capability to transform workflow. Our central lab performs special (histochemical) stains in batches using single positive controls. Special stain control (SSC) slides are manually checked for quality by a technician and the medical director for histology.Stained patient slides (but not controls) are delivered to 4 different hospitals. This project aimed to determine if centralized whole slide imaging could improve pathologist access to control slides without delaying turnaround time (TAT).
Design: Whole slide images (WSI) of special stain control slides were created on an Aperio CS2 scanner within our central histology lab. 226 slides were scanned at 40x (0.25 μm/pixel). WSI were organized on a server according to SSC, date and time of staining, and run indicator. SSC and patient slides were both labeled with the stain run indicator. Pathologists could view WSI for SSC via a link to the server using Webscope/ Imagescope software.
Results: Lab technicians scanned on average 28 control slides per day, divided in AM and PM runs. Of 293 slides, 2% required rescans: 4 Grocott and 1 trichrome due to prescan focus point errors, 1 AFB due to the scanner software not being able to detect the tissue (small size and faint stain). Storage space for the 293 WSI was 28.9 GB. All stain types were easily visualized (including spirochete, gram, and AFB). TAT was improved by 1.65 hours (AM) and 10.5 hours (PM). No connectivity issues were encountered while viewing the WSI. This enabled QA approval of control stains to be accepted digitally in place of glass slides.

Figure 1. WSI database with Date, Time, Special stain, and indicator of run.
Inset: Patient slide with run indicator correlating to control WSI in database
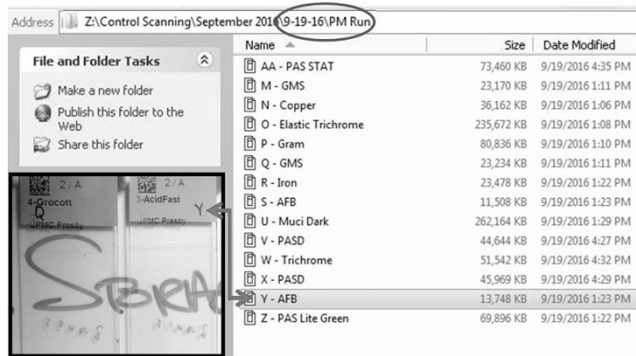
Examples of special stain, tissue section size, and scan time (at 40x)

| Stain	Tissue section (mm)	Avg scan time (min)
Muci Dark	19.2x17.1	20
VVG	15.8x13.6	15
Reticulin	5.4x4.6	6
Iron	4.5x2.1	4

Conclusions: Digitizing glass slides of positive SSC in a multi-site hospital system can improve efficiency, TAT and user access to SSC slides. Incorporating such SSC slides that are not accessioned to patient cases is a unique challenge when implementing a full digital solution in the pathology lab. We developed a custom solution to address this barrier. Digital pathology vendors should consider providing pathology clients with a similar integrated solution to address workflow functionality for control slides.

1589 Advanced Decision Support for Anatomic Pathology Laboratory Information Systems
Douglas Hartman, Michael A Fitzgerald, Anthony L Piccoli, Samuel A Yousem, Liron Pantanowitz. University of Pittsburgh School of Medicine, Pittsburgh, PA.
Background: The practice of pathology is becoming more complex and expensive, especially in regards to ordering ancillary studies and test utilization. National efforts have also been launched to encourage evidence-based medicine and to implement decision support rules within electronic health records. Our aim was to create a tool within our anatomic pathology laboratory information system (APLIS) with customized logic to generate real-time computerized alerts pertaining to diagnostic/therapeutic decision making for the surgical/cyto-pathologist.
Design: With our APLIS vendor (CoPath Plus, Cerner) we customized a rule builder to create alerts that can be filtered by case part type (e.g. biopsy), data field (e.g. process, synoptic information) and value (e.g. specific stain, diagnosis). Figure 1: Screenshot of the rule builder utility in our APLIS.
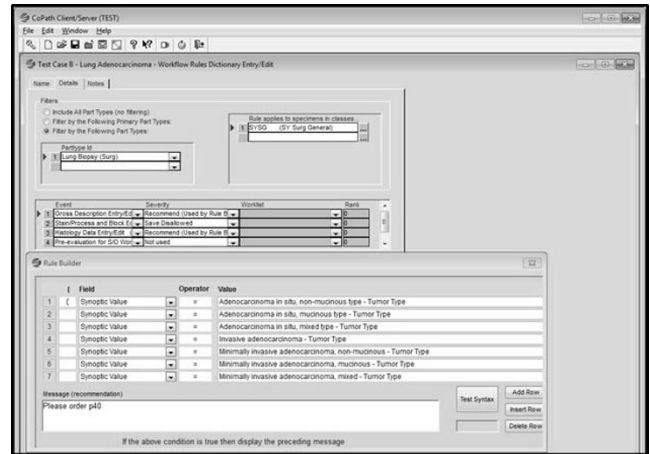
When triggered, these alerts fire within the APLIS containing a message intended to favorably alter and educate the pathology end-user's practice patterns.
Results: Several case scenarios were created to test this tool. Example A: For a gastric biopsy, when a Giemsa stain was ordered, an alert to recommend Helicobacter immunohistochemistry instead was generated. Example B: For a lung specimen with adenocarcinoma, ordering TTF-1 prompted a message to also add p40 and p63. Example C: When signing out a case of colon adenocarcinoma with documented metastasis (stage pM1), the pathologist was notified to order mismatch repair protein and molecular testing.
Conclusions: To the best of our knowledge, such functionality that offers clinical decision support has not been widely incorporated into the APLIS. This tool is highly flexible, allowing us to create any requested rule within the APLIS. These alerts have the potential to standardize care, to force adherence to best practices and to assist our pathologists with many clinical-decision making tasks, such as ordering appropriate ancillary tests.

1590 Creating a Digital Slide Repository: A Novel Educational Tool for Pathology Trainees
Devi Jeyachandran, Brandon Veremis, Abul Ala Syed Rifat Mannan, Pooja Navale, Matthew G Hanna, Tamara Kalir. The Mount Sinai Hospital, New York, NY; University of Pittsburgh School of Medicine, Pittsburgh, PA.
Background: Glass slide repositories/boxes have historically been a major educational tool in Pathology training. However, digital pathology is increasingly becoming an important educational modality, and interpretation of virtual slides has become a component of Anatomic Pathology Board examination. Hence, it is of paramount importance for trainees to be acquainted with this fast-emerging tool. As digital slides can be viewed remotely, they offer an immediate on-demand access to learners. At our institution we sought to create a digital slide repository for resident teaching. We herein summarize our creation of a digital slide repository, as well as its introduction into the pathology educational curriculum.
Design: Residents were assigned to submit glass slides of interesting cases on a weekly basis. Glass slides of cases deemed of educational value (including rarities) were de-identified and scanned using a whole slide scanner and uploaded to slide viewer software. Corresponding de-identified clinical information was also entered. Each trainee was further requested to generate 3- 4 multiple choice questions on the entity along with a brief discussion.
Results: Over a period of 1 year, between September 2015 to September 2016, 265 scanned cases have been uploaded to the image database. Digital slide images were further grouped by subspecialty in separate folders. Each digital slide was given a unique identification number and was saved along with the brief educational material prepared by the trainee. Most of these cases were discussed at a bi-weekly 'Resident Interesting Cases' conference, moderated by an attending. Residents presented the assigned case from the virtual slide repository, and participated in an interactive discussion. The digital slides were available for viewing and residents are allowed access with a unique password protected user id.
Conclusions: The creation of a digital pathology slide repository has allowed us to catalog unique de-identified patient cases. This has qualitatively enhanced the 'Resident Interesting Cases' conference. As digital pathology becomes increasingly utilized in

the diagnostic arena, the availability of a digital skill set during residency assumes more importance. In summary, this modality is readily available, accessible, and gives house-staff greater opportunities to enhance their diagnostic expertise.

1591 Computational Pathology versus Manual Microscopy: Comparison Based on Workflow Simulations of Breast Core Biopsies

Terrell Jones, Luong Nguyen, Akif B Tosun, S C Chennubhotla, Jeffrey L Fine. University of Pittsburgh, Pittsburgh, PA.

Background: Manual review of microscope slides is the standard for pathology diagnosis. Computational pathology techniques now exist which could permit advanced workflows. Featuring automated preview, triage and presentation of diagnostic regions of interest (ROIs) for expert pathologist decisions, this is termed computer assisted diagnosis for pathologists (pCAD). Herein we compare manual slide reviews with simulated computer-assisted reviews, to determine if pCAD could improve pathologist productivity.

Design: An experienced breast pathologist reviewed breast core biopsies (3 H&E levels per block). Audio recordings were analyzed for time measurements including slide movements (i.e. time per ROI/field of view). It was assumed that pCAD could reliably find diagnostic ROIs and that one could view all 3 levels of an area simultaneously onscreen. The 5 longest ROI measurements in each case were assumed to be diagnostic and were used in the pCAD model. Remaining ROIs were assumed to have more rapid review, 0.5s each. Using actual measurements from audio data, simulated pCAD time data was created for each specimen using these assumptions. 2-sample t-test was used to assess results.

Results: Audio data were analyzed, which included a variety of benign, atypical and malignant cases (n=25 cases). Average time to manually review a biopsy case was 221.6s (standard deviation 141.3s). Average simulated time to analyze a biopsy case was 98.0s (standard deviation 50.6s), a statistically significant 55.8% reduction compared with glass (p<.0005).

	Mean	Standard Deviation
Time (glass slides, seconds)	221.6	141.3
Time (pCAD, seconds)	98.0	50.6
Time Saved (seconds)	123.7	
Reduction (%)	55.8%	p=.000266

Conclusions: More than 1 million women receive breast core biopsies in the US yearly, and all of these biopsy slides are manually reviewed. This is a fabulous opportunity for computational pathology; extrapolation of our data suggests pCAD could save more than 50,000 pathologist-hours annually in the US, plus there may be additional benefits such as improved concordance and accuracy of diagnoses. Although pCAD is hypothetical, existing computational pathology pipelines can parse and triage entire slides using spatial statistics and machine learning techniques. Our study is a critical foundation as it provides data about how pCAD workflow could be designed and applied to real diagnostic work.

1592 Live Digital Telepathology Enables Rapid Remote Frozen Section Diagnosis and Cytology Adequacy Assessment by Subspecialists

Yehonatan Kane, Farbod Darvishian, Fang-Ming Deng, Andre L Moreira, Aylin Simsir, Christopher William, Matija Snuderl. New York University Medical Center, New York, NY.

Background: Pathology practice has changed due to the increase of subspecialization, hospital mergers and cost pressures. We sought to evaluate the feasibility of rapid telepathology consultation between a large tertiary medical center and a community hospital in the major underserved metropolitan area for frozen section (FS) diagnosis and cytology adequacy assessment using live digital microscope.

Design: Thirty cases, 20 surgical, 5 cytology, and 5 neuropathology, were selected from previous FS and rapid evaluations and loaded into a Sakura VisionTek live digital microscope at the community hospital as would be for a consultation. Surgical pathology cases consisted of one H&E FS slide per case, and spanned gynecologic, skin, thoracic, breast, head neck, and genitourinary specimens. The neuropathology cases consisted of one H&E FS slide and one H&E stained smear. Each rapid cytology evaluation consisted of one Pap and one Diff-Quik stained slide per case. Five board certified subspecialty pathologists were selected to render diagnoses. Three of the evaluators were surgical pathologists, one a neuropathologist, and one cytopathologist. The evaluators assumed control of the virtual digital microscope remotely by using VNC connection after the slide was loaded and adjust image qualities.

Results: In contrast to a slide scanner, the live digital microscope provided immediate visualization of the slide. Participants reported ease of use by VNC connection, minimal delay and high quality of images comparable to a bright field microscopy. Ninety seven percent (68/70) all diagnoses, all (5/5) rapid cytology evaluations, and all (5/5) neuropathology diagnoses were concordant with the originally rendered diagnoses. One diagnosis involving an inked margin was discordant by two validators and was considered indeterminate after re-reviewing the original FS slide rather than misdiagnosed due to the virtual image quality.

Conclusions: Telepathology is safe and effective method of rendering intraoperative diagnoses and specimen adequacy remotely by pathologists. Immediate visualization and lack of scanning time favors live digital microscopy over a scanning microscope for quick turnaround time. Interpretation of slides via live interactive streaming proved to be comparable from that of a light microscope.

1593 The Use of Camtasia Studio 8 with Narrated Virtual Microscopy as a Multimedia Resource for Pathology Education

Priyadarshini Kumar, Xuemo Fan. Cedars Sinai Medical Center, Los Angeles, CA.

Background: Camtasia Studio 8 (TechSmith, Okemos, MI) (CS8) is a software program that can capture and edit digital recordings of computer monitor outputs with audio narration. It is widely used for instructional purposes in various specialties, however it has received limited interest to teach pathology residents. One-on-one scope time is unique to pathology training and is not easily reproducible. We sought to evaluate the feasibility and usability of this software to create multimedia options for histologic diagnostic learning.

Design: Instructional videos were prepared using CS8 and saved in several databases; department intranet, YouTube.com, Google Drive and Screencast.com [SC] (TechSmith, Okemos, MI). SC was the only interface that permitted restricted access of content to authorized users. Videos included grossing demonstration, didactics and attending-narrated whole-slide images prepared with Aperio scanner (Leica Biosystems, Buffalo Grove, IL). Videos include hyperlinks to supplemental resources and pre&post tests using a cloud based survey tool. A focus group of 10 residents was used to examine the videos and provide feedback.

Did you find these videos useful for pathology learning? (0-5; 0 = not useful 5 = very useful)
What platform was most useful for viewing?
Please rate the overall video quality? (Satisfactory; Unsatisfactory)
Please rate the features of the video (0-5) - Grossing demonstration - Attending-narrated whole slide image - Didactics - Quizzes - Hyperlinks to other resources
What is the most important factor to determine whether your will use these videos to supplement your learning?

Results: The members of the focus group overall liked the technology, rating it very useful (average: 4.8, range 4.0 - 5.0). Residents were satisfied with the video quality, and the length of video was the most important factor in predicting the likelihood of use. Youtube.com was the preferred viewing method. Residents rated the attending-narrated whole slide images an average of 4.8 out of 5; higher than all other listed features. Post test results for junior residents (n=5) showed an average improvement of 1.5 points.

Conclusions: Videos utilizing CS8 which include attending-narrated virtual microscopy slides, hyperlinks to additional materials and quizzes provide an efficient method to supplement the teaching of pathology. As pathology residents are expected to learn an ever-growing body of information in only 4 years, this technology offers an efficient way to disseminate this information in an accessible manner.

1594 Extraction of Machine-Readable Data from Thyroid Fine Needle Aspiration Reports Supports the Need of Structured Data Implementation in Laboratory Information System (LIS) Software

Razvan Lapadat, Christopher Garcia, Bryan Hunt, Tamar Giorgadze. Medical College of Wisconsin, Milwaukee, WI.

Background: The integration of clinical decision support systems into clinical practice is hampered due to a lack of structured, machine-readable data in the existing format of the pathology LIS records. Natural language processing (NLP) algorithms have built-in capabilities for parsing and analyzing free text information into machine readable data. The aim of the current study was to analyze the preparedness of our data in thyroid fine needle aspiration (FNA) cytopathology reports for NLP.

Design: FNA reports of the thyroid were extracted using an LIS software suite (Cerner). The Bethesda System of Reporting Thyroid Cytopathology (TBSRTC) diagnostic categories were used in the stratification of the data set. A natural language open source software tools (R Package) was used to extract information regarding pathologic diagnoses of interest. Data tables were created from the extracted information according to procedure type (assisted vs. unassisted), TBSRTC category, main diagnosis, date of the procedure, site of procedure, operator, patient's age and gender and medical record number. The diagnosis field data was further converted to a data frame and then to a linguistic corpus, which was processed with functions provided in the package *tm*. The corpus data included the stemmed and unstemmed word variants. The variety of ways in which each diagnosis could be represented was recorded, as a means of demonstrating the complexity of machine interpretation of free text.

Results: A number of 3599 thyroid FNA reports out of a total of >25,000 non-gynecologic cytology reports were identified over a period of five years. A widespread variation in the reporting of pathologic diagnoses over the six different TBSRTC categories was seen. The lowest variation was observed for TBSRTC category I (2 different expressions), V (one expression) and VI (one expression). There were, for example, 51 unique ways of expressing entities in TBSRTC category II and 15 unique ways of representing TBSRTC category III. The term-document matrix is composed of 73 unique terms contained in one document. It contained no zero element entries (sparsity 0%).

Conclusions: Thyroid cytopathology diagnostic reports represent a free-text, large body of information that is amenable to machine-readable conversion using NLP tools. Our findings underline the necessity for the implementation of structured data in cytopathology reports, leading to a reduction of the information complexity and chance for error in using NLP.

1595 The Use of Computer Vision to Diagnose Squamous Intraepithelial Lesions of the Lower Female Genital Tract

Xinyan Li, Vassilios Morellas, Nikolaos P Papanikolopoulos, Alexander M Truskinovsky. University of Minnesota, Minneapolis, MN; Roswell Park Cancer Institute, Buffalo, NY.

Background: After successfully using computer vision to diagnose carcinomas of the endometrium, prostate, breast and ovary, and myometrial leiomyomas and leiomyosarcomas, we now turn to diagnosing vulvar and cervical squamous intraepithelial lesions (SILs), infectious and sometimes premalignant conditions of the lower female genital tract. Compared with the above more diffuse diseases, SILs are spatially much more restricted and confined to stratified squamous epithelium. For a human pathologist, the difference between normal squamous epithelium and low- and high-grade SILs (LSIL and HSIL, respectively) lies in the degree of nuclear maturation in the suprabasal epithelial layers, nuclear atypia (enlargement, hyperchromasia, irregular contour), koilocytosis and mitotic activity. Among human pathologists, diagnosis of SILs shows high interobserver variability.

Design: Twenty-two color images of H&E-stained slides of vulvar and cervical biopsies and excisions, scanned on a digital slide scanner at x50 magnification, were manually annotated into normal (14 cases), LSIL (6 cases), and HSIL (16 cases) to train the classification algorithm, then sliced into overlapping blocks of 20x20 pixels (2-19 nuclei per block), yielding 16400 useful blocks for normal, 3486 for LSIL, and 16968 for HSIL. We used Region Covariance Descriptor (RCD) to extract abstract features from the raw image and applied K-nearest neighbor (KNN) search to recognize different types. We selected color features (R,G,B) and texture features, i.e. Ix, Iy (gradient of the image along x and y axis), to construct the RCD. Ten-fold cross-validation was then implemented to evaluate the overall performance of the computer assistant tool on this database.

Results: The precision of computer vision in diagnosing normal squamous epithelium, LSIL, and HSIL was 97.99%, 100%, and 98.56%, respectively. The overall diagnostic accuracy was 98.88%. The accuracy of distinguishing between normal and LSIL, between normal and HSIL, and between LSIL and HSIL was 100%, 98.81%, and 99.71%, respectively.

Conclusions: Computer vision yields excellent results in diagnosing SILs, showing that it can be successfully applied to *in situ* pathologic processes. In particular, its great performance in identifying LSIL, an often contentious diagnosis among human pathologists, is encouraging. Its similar good results with atypical leiomyomas in our previous study raise a question whether computer vision is better than humans at handling borderline diagnostic categories.

1596 Diagnostic Implications of 2-Dimensional and 3-Dimensional High-Definition Videos in Anatomic Pathology

Emilio Madrigal, Shyam Prajapati. Mount Sinai Health System, New York, NY.

Background: Photography is a widely adopted method to create permanent records of specimen features in anatomic pathology. This type of visual documentation is an incomplete and underutilized practice that may limit the ability of pathologists to resolve macroscopic-histopathologic discrepancies. We developed and tested a system to capture and review gross examinations in 2-dimensional (2D) and 3-dimensional (3D) high-definition (HD) platforms.

Design: Two HD camcorders synchronously recorded the gross examination of three uteri. The video files were edited to an average length of 148 seconds and converted to stereoscopic 3D. Four attending pathologists and three residents viewed the videos in 2D on a 22" HD monitor and then in 3D using a virtual reality head-mounted display, after a one-week washout period. Participants measured, oriented and described the color of each specimen; answers were compared to a gross description from a standard prosector. Self-reported motion sickness was evaluated by the standardized Simulator Sickness Questionnaire (SSQ). Utility and opinions of the presented system were assessed by Likert scale questions.

Results: Intraclass correlation coefficient (ICC) for 2D and 3D modalities ranged from 0.6 to 0.97, and a Spearman's rho between the 2D and 3D measurements ranged from 0.57 to 0.92. Bland-Altman plots comparing 2D and 3D to the standard prosector showed differences within 95% confidence interval. 61.9% of participants correctly assessed orientation in 2D and 3D, while the color was accurately interpreted by 71.4% and 85.7% using the 2D and 3D videos, respectively. The average SSQ value before and after the 2D videos was 2.14, while the values before and after the 3D videos were 4.81 and 6.41, respectively. 86% of the participants preferred to have access to full videos during sign-outs of complex cases; 71% would choose videos over photography.

Conclusions: Our system allows trained viewers to confidently assess gross surgical specimens. Our ICC indicates reliable reproducibility of measurements when using the 2D and 3D videos among participants, and there is an excellent correlation between the 2D and 3D measurements. The Bland-Altman plots suggest sufficient agreement between the 2D, 3D, and standard approaches. SSQ results suggest motion sickness was not encountered in either viewing experience. We envision specimen videos becoming multisystem compatible, by being encapsulated with patient metadata and integrated into the AP laboratory information system.

1597 Pathology Informatics 115 Years Ago: Analysis of Surgical Pathology Reports from a University Hospital Surgical Pathology Repertoire in 1901

Martin J Magers, Marina Selenica, Rajan Dewar. University of Michigan, Ann Arbor, MI; Carnegie Mellon University, Pittsburgh, PA.

Background: Surgical pathology (SP) has been practiced since the 1800s. Laboratories functioned for years without the aid of computerized laboratory information systems. In a paper regarding …*The future of Pathology Informatics*, author Jay Hess states, "In 1900, the Laboratory Information System for the University of Michigan was a single leather-bound ledger with handwritten diagnoses." We retrieved several volumes of these ledgers and compared them to present-day SP cases.

Design: Handwritten SP reports from 1901 were examined. Data [age, gender, and diagnosis category (inflammation, infection, neoplasia, or other)] from 131 consecutive SP reports from 1901 were compared to 131 consecutive cases from July 1, 2016.

Results: SP reports in 1901 were neatly handwritten in pen, lacking noticeable errors, with similar format to present-day reports, and hand-signed by a pathologist. Case numbering began July 1 in 1901 (e.g., #1) and January 1 in 2016 (e.g., SU-16-1). Annual SP volume increased from 1901 to 2016 (240 vs >90,000 cases per year). Adult patient age (≥18 years) at the time of SP diagnosis was greater in 2016 (mean: 40 vs 58 years, p-value <0.01). Diagnosis category proportions changed as inflammation decreased (35% vs 14%), infection decreased (14% vs 4%), and "other" increased (3% vs 34%) from 1901 to 2016 while neoplasia was unchanged (48%; p-value <0.01). The proportion of malignant neoplastic diagnoses decreased from 68% (1901) to 58% (2016). "Other" diagnoses in 1901 included ruptured spleen, scar, and normal tissue, while the 2016 cases included such procedures as screening biopsies, reduction mammoplasties, and hernia sac excisions.
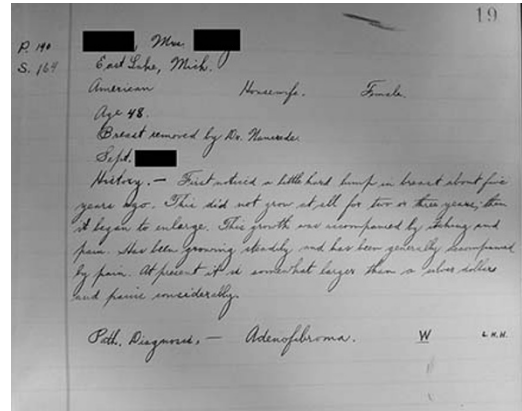
Conclusions: Systematic organization of data was crucial to a university hospital SP practice as early as 1901. July 1 was the start date for numbering SP cases, possibly due to the fiduciary reporting processes in hospitals. The age of adult patients has increased, perhaps reflecting an increase in expected lifespan. While the proportion of neoplastic cases was unchanged (48%), the proportion of cases with infectious/inflammatory diagnoses decreased as modern microbiologic and serologic testing modalities were developed.

1598 WIYDX: A Versatile Interactive Online Platform for Pathology Education

Abul Ala Syed Rifat Mannan, Shyam Prajapati, Emilio Madrigal, Rajendra Singh. Mount Sinai Hospital, New York, NY.

Background: Pathologists, both in residency and in service are overburdened with the daunting responsibility of multitasking as a diagnostician, teacher, and academician. The increasing complexity of multidisciplinary involvement and cognitive data burden is not fully replicated in traditional textbooks, slideshow presentations, websites or journal reports. However, the fast evolving era of digitization offers us a unique opportunity to find a solution to maximize our potentials. Currently, a durable learning resource that can be updated, enhanced, repurposed, and reused digitally does not exist.

Design: We developed a platform (WIYDx.com) to share educational materials. The platform is designed to have ongoing input from renowned authors with the support of multiple interactive features that include: digital slide repository, online presentation platform (pathPresenter.com), gross dissection video library and online lectures/slide seminars (pathCast.net).

Results: The platform is built in a fashion that it can replace current publishing formats and give control of publication to authors rather than publishers. The platform has Chief Editors for each subspecialty who invite other academicians to contribute. The content is in an interactive format where the reader can easily search information at point of need anytime, anywhere. The content includes clinical, macroscopic and microscopic descriptions, with embedded images, dissection videos, and virtual whole slides. Users can upload their own digital slides to the library and use them for content development or presentations. The uploaded slides can be kept for private use or shared in the WIYDx library for anyone to use. Pathology departments will be able to use the services to present tumor boards. The gross dissection library comprises high-definition videos with instructional audio voice-overs. The online lecture series comprises videos of pathology lectures/slide seminars delivered by experts in different fields.

Conclusions: WYDX presents pathology in an innovative interactive format. It is intended to be a platform for pathology learning from world renowned experts that is updated on a continuous basis. This will be useful not only for pathologists but every clinician to maximize their understanding of the subject. This tool can fill the void in underprivileged areas where there is lack of resources and formalized training options. We envision to incorporate online consult services and expand it to include other branches of medicine.

1599   Histological Characterization of Colorectal Polyps Using Deep-Learning

Andrea Olofson, Saeed Hassanpour, Catherine Nicka, Allen Miraflor, Laura Gordon, Saeed Hassanpour, Arief Suriawinata. Dartmouth-Hitchcock Medical Center, Lebanon, NH.

Background: Recent studies have shown that approximately one third of colorectal carcinomas derive from the serrated polyp pathway. Distinguishing between the histologically similar sessile serrated polyps, which have a malignant potential, and hyperplastic polyps, which have no malignant potential, is therefore of considerable import. However, recent studies have also demonstrated considerable interobserver variability amongst pathologists in how they diagnose these two lesions. Considering the significant divergence in patient care following the diagnosis and the challenge in its reproducibility, an alternate approach to assist the evaluation of colonic polyps is warranted. Here, our goal is to develop an accurate automatic method to analyze and characterize the histopathological features of colorectal polyps through the use of deep learning computational model.
Design: Whole slide digital images of hematoxylin and eosin (H&E) stained slides of hyperplastic polyps (HP), sessile serrated adenomas/polyps (SSA/P), tubular adenomas (TA), tubulovillous adenomas (TVA), traditional serrated adenomas (TSA), and normal colonic mucosa were created using the Leica Aperio AT2 scanning system. Cropped images focusing on the histopathological features characteristic of each polyp type were collected and used to build and train a deep-learning image analysis system. To evaluate the feasibility of our approach, an initial pilot study incorporating 1,100 images from the aforementioned polyp types were collected. Of these, 85% were used as a training set, and the remaining 15% were used to evaluate performance.
Results: Initial results from the pilot study evaluating the ability of the computational model to correctly identify polyp type yielded an overall diagnostic accuracy rate of 90.1% (95% CI 84.4%-94.2%). Accuracy rates for the individual categories were as follows: HP 83.9%, SSA/P 85.1%, TVA 91.3%, TA 95.0%, normal 95.0%.
Conclusions: Through the use of high throughput, whole-slide digital imaging and deep-learning computational models, the field of digital pathology is well-poised for the development of an automated method of assisting pathologists in the histopathological analysis of microscopic images. The preliminary results from our pilot study are promising. To further build our image analysis system, the training set will be expanded and tested for accuracy against whole slide digital images.

1600   WSI-FS II: Validation of Squamous Cell Carcinoma Whole Frozen Section Slide Image Diagnosis in Surgical Pathology

Vamsi Parimi, Ryba Dominika, Ewa Borys, Vijayalakshmi Ananthanarayanan, Swati Mehrotra, Xianzhong Ding, Maria M Picken, Dariusz Borys. Loyola University Medical Center, Maywood, IL.

Background: Automated whole slide imaging (WSI) using high-resolution scanners are becoming popular platform in surgical pathology clinical practise for formalin fixed paraffin embedded stained sections but not so for frozen section (FS) diagnostic evaluation. We report results from second validation study cohort demonstrating inter-observer diagnostic variability of WSI- FS squamous cell carcinoma (SCC) slides to that of original glass slide (G-FS) interpretation.
Design: A total of 108 FS SCC cases (218 specimens and 463 glass slides) from random sites from 2013 to 2015 are scanned by Aperio CS2 slide scanner (Leica Biosystems, San Diego, CA, USA). These cases were originally interpreted on glass slides by multiple pathologists. In our study, 6 surgical pathologists independently evaluated WSI-FS slides (including deep cuts) necessary to make a final diagnosis on eSlide Manager (Leica Biosystems) platform. Diagnostic discrepancies were studied at specimen and case level and a consensus was reached. No clinical or prior diagnostic information (age, sex, clinical history, location, presence or absence of tumor) was provided to the pathologist in aiding diagnosis.
Results: Primary neoplasms, margins of surgical resections and lymph nodes specimens to exclude SCC, were the common FS specimens. On an average 12 seconds were spent on each WSI-FS to reach to a diagnosis. The concordance between G-FS and WSI-FS among pathologists A, B, C, D, E and F is as follows:

Total Specimens (n)	246	Pathologists: A,B,C,D,E&F					
Pathologists: A,B,C,D and E	G-FS	WSI-FS (A)	WSI-FS (B)	WSI-FS (C)	WSI-FS (D)	WSI-FS (E)	WSI-FS (F)
Positive for SCC	142	61%	61.30%	50.30%	58%	53%	28%
Negative for SCC	104	39%	38.70%	49.70%	42%	47%	72%
Overall Concordance	% (n)	90% (208)	85% (193)	84% (176)	91% (185)	91% (162)	93% (234)
p value		<0.05	<0.05	<0.05	<0.05	<0.05	<0.05
False Positivity		4.70%	6.70%	0%	0.90%	0%	1.40%
False Negativity		2.50%	6.60%	16.80%	8.90%	8.90%	6%

Conclusions: The concordance between G-FS and WSI-FS interpretations was significantly high. SCC FS diagnosis by WSI was accurate and reproducible. Based on our study, surgical pathologists need additional screen based-training time to gain expertise before utilizing WSI-FS for diagnostic sign-out. We established diagnostic concordance between digital and glass slides by CAP-PLQC recommended guidelines. Our study is the first to specifically evaluate WSI-FS review of SCC; one of the common carcinoma encountered in frozen section surgical pathology service.

1601   Informatics for Prospective Biospecimen Procurement: Performance of a Web-Based Research Tissue Procurement - Information System (RTP-IS)

Anil Parwani, Randal L Mandt, David G Nohle, Leona W Ayers. The Ohio State University, Columbus, OH; Collaborative Human Tissue Network, Columbus, OH.

Background: Research bioinformatics for dynamic, complex, large volume biospecimen prospective procurement (>15K samples/year with associated data) for a variety of basic and translational pre-vetted and approved investigators with individualized biospecimen requests are not commercially available. A **Research Tissue Procurement-Information System (RTP-IS)** was developed in-house using a web based, open source GRAILS Java-based framework with Jasper Reports (TIBCO Jaspersoft), deployed securely inside the medical center fire wall and password protected on the local area computer network
Design: Prospective biospecimen procurement personnel in Investigator Management Service (IMS), Tissue Procurement Service (TPS), Biospecimen Management Service (BMS) with biospecimen transient storage, pathologist quality control (QC) and Billing enter the required data using formatted RTP-IS screens with dropdown menus. RTP-IS management reports are periodically generated to evaluate procurement activity, type and quality of the biospecimens procured and billing activity. Reports were prepared and shared to monitor the adequacy of patient consent process and for regular Quality Improvement activities.
Results: RTP-IS activity reports documented 11,812 biospecimen procurement opportunities with 21,160 samples procured from 4,236 distinct patients in 28 months. The QC pathologist reviewed 4,960 QC samples with <5% failing review. 18,505 samples were shipped and billed to 263 investigators for 663 study requests. Procurement technologists identified surgeries and used RTP-IS to track them for tissue collection, enter and manage data associated with: tissue collection based on investigator tissue requests, consent status, QC, chart review/specimen distribution, billing and accounts receivables. RTP-IS provided extensive, secure data storage, data analysis and management statistical reports required by research funding.
Conclusions: The RTP-IS is a robust web-based tool that not only provides comprehensive, secure data storage, data analysis but also provides a unique platform for enabling collaborative research. Informatics brings discipline to improve a large, complex and dynamic prospective tissue procurement program and facilitates integration of dynamic activities into activity reports to guide resource deployment for ongoing basic and translational research.

1602   Specimen Tracking Using Two-Dimensional Barcode System for Anatomic Pathology

Anil Parwani, Keluo Yao, Lindsay Thorn, Sandra Banky, Keith Mullins, JoAnna Williams, Adrian Suarez. The Ohio State University Wexner Medical Center, Columbus, OH.

Background: Traditional one-dimensional (1D) barcode system has low information density and is subject to some instrument read errors. Up to 1 in every 88000 scans can be an error from a 1D system. Very few institutions have implemented a department-wide two-dimensional (2D) barcode system with a unique serial number for each container/cassette/slide. The aim of this study was to detail the experience of implementing such a system at a large academic institution.
Design: We obtained ID/Positive™ CL-04 Laser Cassette Printer system with Global Standard One (GS1) 2D barcode system and ID/Positive CL-Series Tissue & Biopsy Cassettes (General Data, Cincinnati, OH). The anatomic pathology laboratory information system (APLIS) was updated to CoPathPlus Version 6.1 with barcode support (Sunquest Information Systems, Tucson, AZ). The system provides each container/cassette/slide with a unique serial number. Specimen Point of Tracking (SPOT) was assigned for specimen storage, gross room, histology, immunohistochemistry, and individual resident/pathologist to track the status/whereabouts of each specimen. The scanning of the barcode is accomplished with Honeywell Xenon 1900 Handheld 2D Imager Scanner (Honeywell, Morris Plains, NJ) installed at every SPOT location. Tracking is enforced through the use of asset matching/reconciliation (AMC) function of CoPathPlus. The first implementation phase targeted gross room and histology areas.
Results: We have developed a robust infrastructure to track pathology specimen and to prevent mislabeling. In the gross room, the barcode system will minimize mislabeling of cassettes/containers. Tissue switching between different parts/cases could also be reduced. In histology, mislabeled slides and switched tissue sections between different parts of the same/different cases will be mininized. Additionally, due to higher information density, the 2D barcodes have some data redundancy and are damage resistant. The survivability of the specimen labels will be higher and technical glitches associated with barcodes will be minimized.
Conclusions: The 2D barcode system represents the next step in improving the accuracy of specimen tracking in anatomic pathology. We will continue with the implementation of the system and report any performance data in the future.

1603   Identifying the Histomorphometric Basis of MRI Radiomic Features in Distinguishing Gleason Grades of Prostate Cancer

Gregory Penzias, Asha Singanamalli, Robin Elliott, Jay Gollamudi, Natalie Shih, Michael Feldman, Phillip D Stricker, Warick Delprado, Sarita Tiwari, Maret Bohm, Ann Maree-Haynes, Lee Ponsky, Pallavi Tiwari, Satish Viswanath, Anant Madabhushi. Case Western Reserve University, Cleveland, OH; University of Pennsylvania, Philadelphia, PA; St. Vincent's Prostate Cancer Clinic, Sydney, NSW, Australia.

Background: Radiomics involves extracting quantitative features from medical images for improved disease characterization. Similarly, pathomics utilizes computer-extracted histomorphometric (QH) features to characterize tissue appearance on digitized histology. In this work we seek to understand in terms of QH features, the morphologic basis of radiomic features on MRI that are predictive of Gleason score of prostate cancer (PCa).
Design: On a cohort of 36 patients from 2 different sites (23 for training, 13 for validation), pre-operative T2w MRI was co-registered with digitally reconstructed H&E-stained radical prostatectomy sections. Comprehensive sets of 828 QH and 2001 radiomic features were then extracted and spatially co-localized within each tumor region. We then identified the set of (a) radiomic features most discriminating of low vs. intermediate/high grade PCa, (b) QH features correlated with the most discriminating radiomic features previously identified, and (c) evaluated the discriminative ability

of QH features found to be correlated with radiomic features. Multiple hypothesis correction of Spearman's correlation coefficient p-values obtained in step (b) was performed using false discovery rate.

Results: Gland lumen shape features were found to be significantly correlated with a Gabor texture feature.

Conclusions: Our results suggest that the PCa grade discriminability of Gabor features may be a consequence of corresponding grade-related variations in gland shape and morphology at the tissue level (Figure 1).
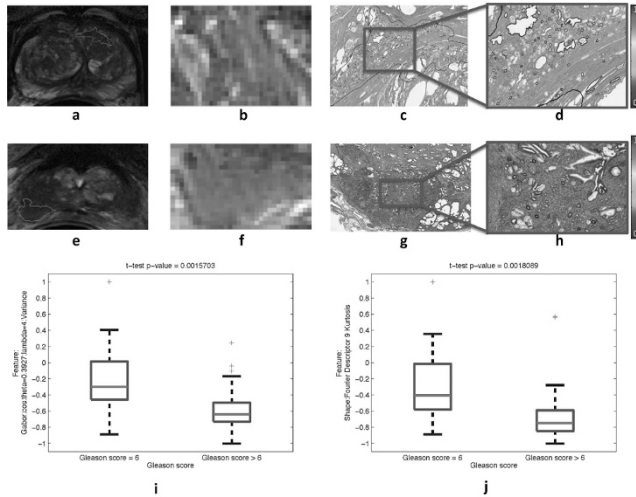

Figure 1: Differential expression for a radiomic and QH feature between tumors with Gleason score 6 (a-d) and 9 (e-h) from the training set. Feature values are plotted within the tumor (blue = low values, yellow/red = high values) shown in the prostate (a,e) as well as zoomed-in (b,c,d,f,g,h). Boxplots summarizing the differential expression of these features over all tumors from the training set are plotted (i, j). Note the low number of colors in the tumor with high (f) relative to low (b) Gleason score, indicating lower variance of the depicted Gabor feature within the high Gleason score tumor.


1604   Error Reduction of Misidentified Paraffin Blocks Through the Use of Automated Cassette Labeling: A Three Year Follow-Up Study

Christine Rupcich, Alaa Alsadi, Diana Murro, Arlen Brickman, Erika Paulsen, Mark Jaros, Shriram Jakate. Rush University Medical Center, Chicago, IL.

Background: Surgical pathology specimens and sampled paraffin blocks are identified by unique assigned alpha-numeric characters entered in and generated by the laboratory information system (LIS). Misidentified blocks are a potential source for errors that can lead to misdiagnoses and compromise patient safety. Our institution (a tertiary care academic center) switched from a manual cassette printer (MCP) to an automated LIS integrated cassette printer (ACP) two years ago (late 2014). We performed a 3-year study spanning roughly one year of MCP and two years of ACP to determine if this replacement led to error reduction.

Design: We reviewed all of our January to June daily quality control log sheets and LIS generated block counts for 3 years (2014-2016) to investigate misidentified blocks. These misidentified blocks were then classified into the following categories: mislabeled, not entered in LIS/deleted in error, surplus/not deleted, missing, blocks with no category, and other. Among these, the mislabeled blocks were considered the most serious type of misidentification with maximum potential for misdiagnoses.

Results: The overall percentages of misidentified blocks decreased every year as follows: 2.86% in 2014 (MCP), 1.06% in 2015 (ACP), and 0.73% in 2016 (ACP). The most common class of misidentification while using the MCP (2014) was "not entered/deleted in error" (67%) and mislabeled blocks were 21% (serious error). After the ACP was installed, along with the overall decrease in misidentified blocks, mislabeled blocks dramatically decreased to only 2%. With ACP, the most frequent misidentification was "surplus/not deleted" (55% in 2015 and 43% in 2016).
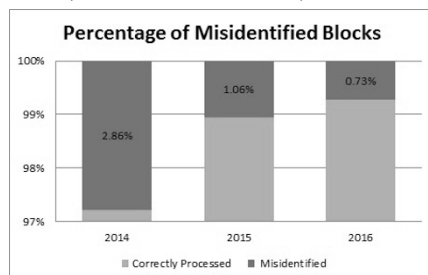
Conclusions: The overall percentage of misidentified paraffin blocks dropped with the use of the ACP (2.86% in 2014 to 0.73% in 2016). Furthermore, there was a dramatic decrease in the frequency of serious type of misidentification such as mislabeled blocks with the use of ACP. Although overall reduced, less serious types of misidentification continued with ACP, mainly in the form of surplus/not deleted blocks. While automated cassette labeling resulted in error reduction and improved patient safety, errors were not completely eliminated.

1605   Utilization of Computer-Verified Training Sets in Ki67 Assessment of Neuroendocrine Tumors

Evita Sadimin, Wenjin Chen, Natalie Gilbert, Nicola Barnard, Marina Chekmareva, Michael May, Parisa Javidian, Sumi Thomas, Malik Deen, David Foran. Rutgers Cancer Institute of New Jersey, New Brunswick, NJ; Rutgers Robert Wood Johnson Medical School, New Brunswick, NJ.

Background: The World Health Organization (WHO) grading system of neuroendocrine tumors (NETs) is based on the mitotic count and Ki67 proliferative index. By Ki67 proliferative index, well-differentiated NETs are divided into low grade G1 (Ki67 proliferative index <3%) and intermediate grade G2 (Ki67 proliferative index 3%-20%). The percentage is determined by scoring 500-2000 cells in areas of strongest nuclear positivity (hot spots). Assessment of this percentage is challenging, with previous studies showing variable reproducibility depending on the specific methods used.

Design: Four color-printed, computer-verified "gold-standard" training sets were created, with each set consisted of four 20X images of Ki67 immunostained slides, representing 1%, 2%, 3% and 4%. Computer verification was performed using digital image analysis (DIA) with a robust execution pipeline specifically developed for the project. This protocol excluded stromal cells and lymphocytes. Pathologists were asked to (1) score a unique set of 20 designated areas on Ki67 immunostained slides using the microscope and (2) score another unique set of 20 JPEG images of Ki67 immunostained slides photographed under 20X on the computer. The four training sets were made readily available to study participants throughout the assessment as reference. The scores were then compared with those obtained by DIA.

Results: The computer-verified training sets were beneficial in both microscopic and computer-based assessments. The computer-based assessment showed better accuracy when compared to the traditional microscopic assessment. In addition, computer-based assessment was faster and more reproducible than microscope assessment. Pathologists were most accurate in assessing cases with 1% Ki67 proliferative index, followed by 4% and 2%. Pathologists were least accurate in assessing cases with 3% proliferative index.

Conclusions: In institutions where DIA is not readily available or is not practical for Ki67 proliferative index assessments in NETs, utilizing training sets is helpful for both assessments using the microscope and on the computer. However, even with utilization of the training sets, scoring photographed images while viewed on a computer screen was still superior to scoring using only the microscope.

1606   PathCaseShare: A Web-Based Pathology Case Sharing Platform and Crowd-Sourced Knowledge Base

Jung Hoon Son, Anthony Rubino, Anna Lee, Shane Betman. Columbia University, New York, NY.

Background: For pathologists willing to share images and information of interesting cases with colleagues and/or the online community, the only reliable web-based platforms available currently are general social media platforms such as Twitter and Instagram. These platforms, however, are designed primarily for simple viewing of the cases. These platforms lack the capability to extract and collect useful data relevant to pathologists to provide aggregated user-oriented (i.e. ability to view distribution of cases uploaded by a user) or knowledge-oriented metrics (i.e. which cases stain positive for CD30?). Despite the extra efforts made by the user to submit the metadata (stain information, clinical history, gross description) onto generic social media platforms, most of the information is lost, which could have potentially contributed in collective building of a pathology knowledge resource. An online case-sharing platform specifically designed for pathology is needed for this reason.

Design: The goal of this project was to create a pathology-specific platform where pathology cases can easily be shared. The platform's design goal is to facilitate sharing of pathology cases through an online interface and construction of a unique knowledge base consisting of crowd-sourced, aggregated pathology case data. A commonly used web programming framework, Ruby on Rails, was utilized to create a web-based case sharing platform specifically designed for pathology cases. The server resides on a secure cloud-based hosting platform (Heroku) and the image data were programmed to be directly uploaded to a cloud-based storage (Amazon S3). Three pathology residents at intermediate level of training (two PGY-2 and one PGY-3) at Columbia University (AL, AR, SB) volunteered in the testing of the platform, along with the initial collection and curation of cases.

Results: PathCaseShare (PathCaseShare.com) is currently available as a beta-service, open for free registration for any users willing to share pathology cases. In addition to being able to sharing/viewing cases, current implemented features include 1) viewing top-rated cases based on categories, 2) convenient compilation of stain profiles of uploaded cases, and 3) crowd-curation of best cases based on other user votes.

Conclusions: A case-sharing platform PathCaseShare has a potential to become as a dynamic pathology knowledge resource. Additional features are planned for the future, based on user suggestions and available resources.

1607   Computerized Density Estimation of Tumor-Infiltrating Lymphocyte in H&E TMAs Predicts Recurrence in Early Stage Non-Small Cell Lung Cancer

Xiangxue Wang, German Corredor, Eduardo Romero, Andrew Janowczyk, Yu Zhou, Michael C Yang, Vamsidhar Velcheti, Anant Madabhushi. Case Western Reserve University, Cleveland, OH; Universidad Nacional de Colombia, Bogota, Colombia; Cleveland Clinic Foundation, Cleveland, OH.

Background: Post-surgery recurrence is a key reason for treatment failure in early stage non-small cell lung cancer (NSCLC), which accounts for 80% of lung cancers. Studies have shown that a high density of Tumor-infiltrating lymphocytes (TIL) are associated with improved survival for certain cancers. However TIL counting and grading is performed manually and hence is subject to inter-observer disagreement. In

this study, we created a fully automated algorithm to quantitatively characterize spatial architecture and density of lymphocytes based on digital H&E images and show their utility in predicting recurrence in early stage NSCLC.

Design: Two independently collected tissue microarrays (YTMA140, n=70 and YTMA79, n=119) were employed in this study. YTMA140 was used to build the machine learning classifier for predicting recurrence and YTMA79 was used for independent validation. All cells were initially segmented using a watershed algorithm. Next, shape and color features (e.g., median red channel value), were employed to identify lymphocytes. Lymphocyte clusters were then constructed using each lymphocyte as a vertex of a graph and the distance between them as edge values. The mean/max lymphocyte density of each cluster was then extracted and used to train a classifier to predict recurrence in early stage NSCLC using YTMA140. YTMA79 was used for independent validation.

Results: The most discriminative features for this task included the max and mean lymphocyte density of all clusters. These features are in concordance with known biological underpinnings of NSCLC. Quadratic Discriminant Analysis yield an accuracy of 0.69, and AUC=0.69 on training set and accuracy of 0.7, and an AUC=0.68 on the independent validation set. Patients with higher TIL density showed a statistically significant (Kaplan-Meier p-value=0.0002) correlation with better outcome as measured by increased disease free survival time (figure 1) on the validation set.
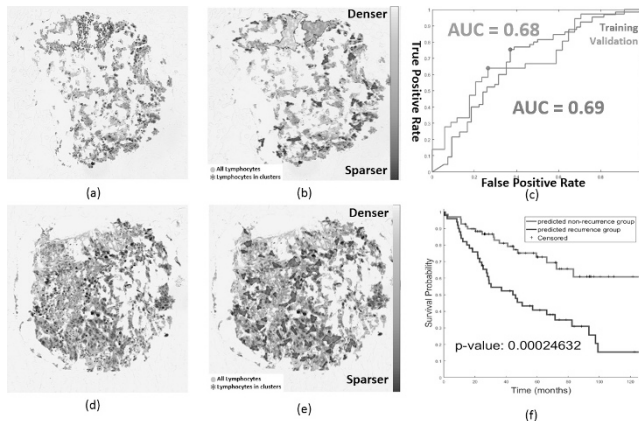

Figure 1. (a) sample of non-recurrence patient; (b) clusters of lymphocytes and densities; (c) receiver operating curve for both training and validation set; (d) sample of recurrence patient; (e) clusters of lymphocytes and densities; (f) Kaplan-Meier estimate by Automatic TILs evaluation model

Conclusions: We presented an automated TIL quantification model that was able to distinguish NSCLC patients with early recurrence from those with longer disease free survival times.

1608 The Use of Screencasts with Embedded Virtual Microscopy Slides and Videos Describing How to Gross Specimens and Narrated Lectures to Teach Pathology Residents

Mary Wong, Alberto M Marchevsky. Cedars-Sinai Medical Center, Los Angeles, CA.

Background: Screencasts, also known as video screen capture, are digital recordings of computer screen outputs with audio narration. They are widely used for instructional purposes in other medical specialties and various industries but there has been limited interest at using them to teach pathology residents.

Design: Screencasts were prepared using Camtasia Studio 8 (TechSmith, Okemos, MI) and Powerpoint 2016 (Microsoft, Redmond WA) software and saved in the departmental website, YouTube.com, Vimeo.com and Screencast.com. They include videos with instructions to gross specimens, case studies prepared with virtual microscopy and narrated lectures. The case studies include a narration of clinical history and radiologic images, hyperlink to virtual microscopy slides prepared with Aperio scanner (Leica Biosystems, Buffalo Grove, IL), a quiz, narrated description of the virtual slide by an attending explaining how to examine the case and a final quiz. Narrated lectures include hyperlinks to supplemental learning materials and quizzes. Screencasts can be viewed with PC or MacOS computers and/or iOS or Android mobile devices. Results of quizzes are automatically emailed to an attending pathologist to monitor progress. A focus group of 11 residents was asked to examine the screencasts and provide feedback to various questions using a 0-5 scale.

Results: Screencast files were relatively small, up to 50 megabytes for videos lasting up to 10 minutes, and could be viewed with a browser using all devices. YouTube.com allowed unlimited free space for videos lasting up to 20 minutes. Screencast.com and Vimeo.com allowed only 2 gigabytes and 25 gigabytes, respectively, at no cost. Only videos saved in Screencast.com allowed for the use of quizzes using proprietary software. Residents provided positive feedback with 4.2 to 4.7 satisfactory ratings to various questions. They favored viewing short videos (up to 10 minutes) using computers rather than mobile devices.

Conclusions: Screencasts that include embedded virtual microscopy slides, hyperlinks to additional teaching materials and quizzes provide an efficient method to supplement the teaching of pathology, providing residents with exposure to interesting cases, lectures, and procedures to gross specimens. They may stimulate learning and allow for monitoring progress using automatic emails. As pathology residents are expected to learn an ever-growing body of information in only 4 years, this technology offers a potentially useful and efficient learning tool.

1609 Computational Image-Analysis to Distinguish Well-Differentiated Hepatocellular Carcinoma from Normal Liver Tissue

Rong Xia, Yongsheng Pan, Amir M Boroujen, M A Haseeb, Raavi Gupta. SUNY Downstate Medical Center, Brooklyn, NY.

Background: Distinguishing well-differentiated hepatocellular carcinoma (WD-HCC) from other hepatic lesions is challenging because of morphologic similarities between them. Computational image-analysis offers new opportunities for objective diagnosis through quantitative assessment of histological features. Here, we have used automatic image processing and statistical analysis to differentiate between the WD-HCC and normal liver tissue (NLT).

Design: Twenty core liver biopsy specimens (11 WD-HCC; 9 NLT) were retrieved and re-evaluated. Images (98 WD-HCC; 97 NLT) were obtained at 400x from non-overlapping areas in H&E stained slides, excluding areas with inflammation, steatosis, cholestasis, artifacts, and portal triads. The computer was trained on 47 WD-HCC and 47 NLT images by classification algorithm for computational image analysis. The remaining images (51 WD-HCC; 50 NLT) were used to test the algorithm. Images were deconvoluted to subtract background colors. After noise reduction and Otsu thresholding, morphologic opening and connected component analysis were applied to enumerate the number of nuclei.

Results: There were greater number of nuclei in WD-HCC as compared to NLT (463.4±84.0 vs. 278.5±32.5; p<0.001). Applying these data from test cases an ROC was developed using binary classification. The remaining images (51 WD-HCC; 50 NLT) were tested by the binary classification algorithm. This computational image analysis differentiated WD-HCC and NLT with a sensitivity of 98% and specificity of 96% with a Kappa coefficient of 0.94.

Conclusions: Computational image analysis of nuclear density differentiated WD-HCC from NLT. The nuclear density was significantly higher in WD-HCC than in NLT. Computerized image analysis can be used to assist in the diagnosis of hepatocellular carcinoma especially in suboptimal specimens.

1610 Validation of Fine Needle Aspiration Rapid Onsite Evaluation Using VisionTek Live Digital Microscope

Keluo Yao, Zaibo Li, Anil Parwani, Rulong Shen. The Ohio State University Wexner Medical Center, Columbus, OH.

Background: Remote assessment of fine needle aspiration rapid onsite evaluation (FNA ROSE) using telecytology has not gained wide acceptance. Remote digital photomicroscopy solutions such as NetCam has limited image quality and end user experience. Recently VisionTek Live Digital Microscope (VLDM) (Sakura, Japan) has been introduced which allows live view and control of cytologic smear through a remotely accessible robotic microscope and advanced image processing software. The aim of this study was to detail the experience of validating VLDM for FNA ROSE.

Design: Sixty FNA cases from lesions of thyroid (16/60), lymph nodes (16/60), pancreas (9/60), head & neck (9/60), salivary gland (5/60), lung (4/60), and rectum (1/60) from 2014 to 2016 were assembled based on routine cytopathology workflow. One representative Diff-Quik stained slide was selected for each case. Thirty cases (30/60) contained neoplasm and the remaining contained benign tissue (24/60) or non-diagnostic materials (6/60). Two board-certified cytopathologists (A and B) independently reviewed the all the slides twice using Diff-Quik optimized VLDM via Webex (Cisco, San Francisco CA) and conventional light microscopy (CLM). A "washout" period of at least fourteen days was placed between the two reviews.

Results: The concordance rate between VLDM and CLM was: 1) 96% for preliminary adequacy assessment (PAA); 2) 82.5% for final diagnosis (FD), adjusted for equivalent nomenclatures; 3) 83% for clinical management (CM), adjusted for clinical decisions based on final diagnosis. The concordance rate of CLM between the two cytopathologists was: 1) 93% for PAA; 2) 87% for FD; 3) 83% for CM. Figure 1 compares unsatisfactory, benign, atypical, and neoplastic/suspicious rates of CLM vs VLDM for each cytopathologist. The average time spent per slide was 270 seconds for VLDM (range: 60 to 1200 seconds) and 113 seconds for CLM (range: 60 to 600 seconds).

		Unsatisfactory	Benign	Atypical	Neoplastic/suspicious	Total
VLDM	Unsatisfactory	10/7	1/0			
	Benign	0/2	20/15		1/3	
	Atypical	0/1	0/1	0/1	0/1	
	Neoplastic/suspicious		0/1		28/28	
	Total					60/60

Figure 1. Unsatisfactory, benign, atypical, and neoplastic/suspicious rates of CLM vs. VLDM for cytopathology A (red) and B (black)

Conclusions: Our data demonstrate that VLDM via Webex is suitable for FNA ROSE to provide precise adequacy assessment and reasonable preliminary diagnosis. Discordant preliminary diagnoses are likely the result of inter- and intra-observer variability. Although some challenges remain regarding speed, throughput, and end user adaptation of the technology.

1611 Remote Neurosurgery Intraoperative Consultation by Visiontek Live Digital Microscope and Webex

Keluo Yao, David A Kellough, Scott Hammond, Scott L Wade, Lynn Schoenfield, Norman Lehman, Adrian Suarez, Anil Parwani, Jose Otero. The Ohio State University Wexner Medical Center, Columbus, OH.

Background: Increase the accessibility of neuropathologist for intraoperative consultation (IOC) of neurosurgery is in the interest of better patient care. VisionTek Live Digital Microscope (VLDM) technology (Sakura, Tokyo, Japan), when coupled with a remote interface (RI), can reduce travel for offsite neuropathologist, allowing IOC to be reviewed by the otherwise inaccessible experts. The aim of this study was to document our experience implementing VLDM using Webex (Cisco, Milpitas, California) as the RI.

Design: We installed a VLDM in the frozen section office. Access was provided to pathologists on their home/office computers via uniquely generated WebEx remote desktop link. Once connected, the pathologists have full control of all the VLDM capabilities, including magnifications, focus, field of view, brightness, linear/nonlinear color corrections, etc. We complied with the 2015 College of American Pathologist Laboratory General Checklist six standards for telepathology (figure 1). Two off-site board-certified neuropathologists (A and B) were trained and then went live with neurosurgery IOC with either traditional travel on-site method or via VLDM/Webex. The final diagnoses (FD) were rendered using traditional methods by the two neuropathologists at a later time.

GEN.50057	Slide Image ID	Slide label appears on-screen. A pathologist is in direct communication with PA or resident.
GEN.50614	Clinical Information Access	Documentation is scanned and placed on the desktop. A pathologist is in direct communication with PA or resident.
GEN.51728	Telepathology Training	Before use, pathologists must undergo training and pass a test demonstrating their ability to diagnose using the system. Equipment and connection pathologist will use must also be vetted. Specific and detailed SOPs are at hand.
GEN.52842	Patient Confidentiality	The session is by invite only from PA or resident to the pathologist. No permanent image is retained.
GEN.52850	Results Documentation	Pathologist signs out digitally. Formal sign-out happens at next earliest opportunity.
GEN.52860	Quality Management Program	Machine receives all required manufacturer maintenance. The system is validated with 60 slide test for each tissue type (conducted in conjunction with Xifin). A Log is maintained of all problems and corrective actions. Day-to-day department QA procedures.

Figure 1. Compliance with College of American Pathologist Laboratory General Checklist six standards for telepathology

Results: Fifty-one neuropathology cases with IOC from June to August 2016 were reviewed. Eighteen cases (18/51) had IOC performed via VLDM/Webex starting middle of July. For all cases, the FDs were compared with the IOC diagnoses. The VLDM/Webex IOC and FD concordance was 94% (17/18), after adjustment for equivalent nomenclatures/management. The on-site IOC and FD concordance was 87.9% (29/33). The average turnaround time (TAT) for VLDM/Webex IOC was 30.6 minutes (range 16 to 45 minutes), on-site IOC 27.3 minutes (range 16 to 49 minutes), and P value 0.11. Neuropathologist A has performed all the VLDM/Webex IOC diagnoses while neuropathologist B continued to perform all IOC by traveling on-site.

Conclusions: The VLDM/WebEx system offers a way to increase the accessibility of neuropathologist for IOC for neurosurgery. Preliminary data shows it has comparable diagnostic and TAT performances to the traditional on-site evaluation and is therefore an easy, reliable, and convenient alternative.

1612 Identification of Cancer Cases Using ICD-9 and ICD-10 Codes in Electronic Health System

Lei Zhang, Javier Sanz, Alexander Stanoyevitch, Robert Follett, Douglas Bell. Anaheim Regional Medical Center, Anaheim, CA; UCLA, Los Angeles, CA; California State University-Dominguez Hills, Carson, CA.

Background: Accurate identification of cancer patients in the existing records is critical for patient care and research. ICD and SNOMED codes are authoritative tools for disease identification, besides their association with claims and reimbursement. We aim to explore how ICD-9 and ICD-10 codes capture the cancer diagnoses in electronic health system.

Design: The study cohort includes 205,952 patients older than 50, with at least two ambulatory encounters from 1/1/2012 to current in UCLA healthy system. The ICD-9 to ICD-10 conversion is automatically performed by Epic EHR system starting 10/1/2015. Cancers are sorted using combined ICD-9, ICD-10 and SNOMED codes. The data are created in CSV files and analyzed using R language.

Results: The combined codes recovered 6328 breast cancer, 416 stomach cancer, and 610 uterus cancer diagnoses in 7281 patients in 3.6 years. Among them, 6 cancer cases have only SNOMED code without ICD codes. The ICD-9/ ICD-10 code identified 82%/15%, 76%/5% and 56%/37% of breast, stomach, and uterus cancer cases respectively. There are only 10%, 3% and 11% of breast, stomach and uterus cancer cases coded by both ICD-9 and ICD-10. Similar results were received for cancers diagnosed within one year of encounter. The repeated findings suggest a small portion of cancer cases have both ICD-9 and ICD-10 codes, corresponding to new installation of ICD-10 system.

CANCER TYPE	INCIDENCE*	TOTAL	ICD-9 DIAG	ICD-10 DIAG	BOTH
TABLE 1A: OVERALL PATIENT COUNTS OF ICD DIAGNOSES IN 3.6 YEARS					
BREAST	3%	6328	5157(82%)	948(15%)	657(10%)
STOMACH	0.2%	416	318(76%)	21(5%)	13(3%)
UTERUS	0.3%	610	339(56%)	223(37%)	64(11%)
TABLE 1B: PATIENT COUNTS OF ICD DIAGNOSES WITHIN FIRST YEAR OF ENCOUNTER					
BREAST	2.3%	4828	3958(82%)	277(6%)	72(2%)
STOMACH	0.2%	374	288(77%)	9(2%)	3(1%)
UTERUS	0.2%	472	269(57%)	96(20%)	15(3%)
* incidence = total cancer cases identified by combined ICD-9, ICD-10, SNOMED / 205,952 (cohort size)					

Conclusions: ICD codes are efficient in identifying cancer cases; but combined use are necessary for a comprehensive recovery of cancer cases in historical database.

1613 Using Machine Methods to Score Tumor-Infiltrating Lymphocytes in Lung Cancer

Tianhao Zhao, Le Hou, Vu Nguyen, Yi Gao, Dimitris Samaras, Tahsin Kurc, Joel Saltz. Stony Brook University, Stony Brook, NY.

Background: There is increasing evidence for the clinical relevance of tumor-infiltrating lymphocytes (TILs). However, pathologists usually score TILs on hematoxylin and eosin (H&E) stained slides, which is subjected to inter- and intra-observer variations. We developed a computer algorithm to classify TILs at an image patch level, which when aggregated, can estimate the % of lymphocyte infiltration in the tumor area.

Design: We used Convolutional Neural Networks (CNN) to classify image patches from lung adenocarcinoma digital slides as either high or low number of TILs. We used 176 whole slide images (WSIs) from 157 patients from the Cancer Genome Atlas repository. A pathologist classified 22267 image patches of 100x100 pixels at 20x. We trained our CNN on this dataset and millions of unlabeled patches in a semi-supervised fashion. We first trained an unsupervised convolutional autoencoder (CAE) without ground truth labels to capture the features of the lymphocytes. The CAE is trained to detect and represent the nuclei by a set of feature vectors with 100 dimensions (fig 1, A-C). We then initialized a supervised CNN with the parameters learned by the CAE to transfer the knowledge gained. Finally, we trained the CNN on the labeled training set (fig 1, D-E). We evaluated our trained CNN on a reserved testing dataset with ground truth labels.
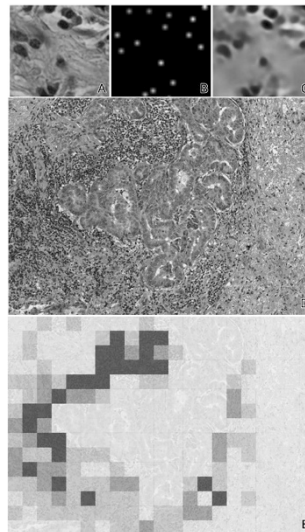

Figure 1: (A)H&E (B)detected nuclei locations (C)reconstructed image (D)H&E of lung adenocarcinoma (E)Heatmap overlay of the image with red and white indicating high and low TILs respectively

Results: We achieved better results compared to using a VGG16 network. The receiver operating characteristic curve for our model showed an area under the curve of 95% for TILs classification (fig 2).
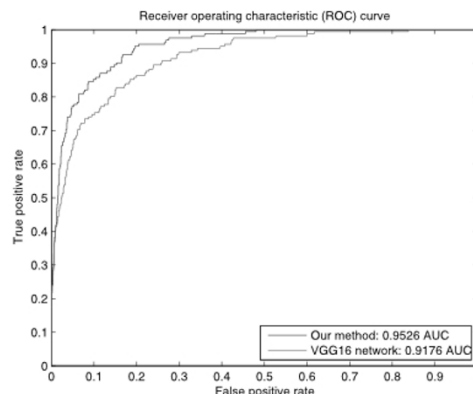

Figure 2 ROC curve

Conclusions: Our method can detect TILs accurately in lung adenocarcinoma. We will deploy and test the method against other cancers in the near future. We hope our machine method can aid pathologists in the evaluation of TILs in cancers.